

THE CONDITIONAL FOOTPRINT OF LARGE AND VERY-LARGE SCALE MOTION IN TURBULENT CHANNEL FLOWS

H. C. H. Ng¹, J. P. Monty¹, N. Hutchins¹, M. S. Chong¹ and I. Marusic¹

¹ *Department of Mechanical Engineering
The University of Melbourne Victoria 3010, AUSTRALIA*

h.ng4@pgrad.unimelb.edu.au

Abstract

This paper will detail experiments conducted using an array of multiple wall skin friction sensors employed simultaneously with a wall normal traversing hot-wire to capture the ‘footprint’ of large scale motions in a turbulent channel flow. It is shown that these very large scale structures extend all the way to the wall and are influenced by (or influence) the behaviour of the wall shear stress. Experiments are carried out at a Reynolds number of $Re_\tau = 1000$.

1 Introduction

The presence of coherent large scale features in turbulent boundary layer, pipe and channel flows is well documented. Hot-wire and hot-film anemometer measurements offered initial insights into the size and structure of the coherent flow features in a turbulent boundary layer. Numerous studies, for example, Brown & Thomas (1977) and Wark & Nagib (1991), compute the two-point spatio-temporal correlation of the stream-wise velocity and wall shear stress and infer the size and angle of the large scale coherent flow features.

The advent of Particle Imaging Velocimetry (PIV) allowed researchers to paint an ever clearer and more intricate picture of the large scale motions found in canonical turbulent flows. However, the interaction between wall shear stress and the largest scales of motion remained unclear owing to the limited resolution of PIV near the wall and the limited field of view, which in turn limited the streamwise extent of the velocity fields (in most cases, $1 - 2\delta$, where δ represents the outer length scale and is the boundary layer thickness, pipe radii or channel half-height depending on the flow geometry).

Pre-multiplied energy spectra of streamwise velocity from single point measurements in pipe, channel and boundary layer flows revealed a bi-modal distribution of the energy. The largest streamwise length scales, or wavelengths, λ_x , were in excess of

$\lambda_x = 12\delta$ for pipe (Kim & Adrian 1999 and Guala, et al. 2006) and channel flows (Balakumar & Adrian, 2007) and up to $\lambda_x = 6\delta$ for boundary layer flows (Hutchins & Marusic 2007a). The maximum stream-wise length scales were shown to exist predominantly in the logarithmic regions of these flows.

To ascertain the span-wise sizes of these large scale events, hot-wire rake measurements were conducted, and instantaneous velocity fields inferred using Taylor’s hypothesis for boundary layers (Hutchins & Marusic 2007a) and pipes/channels (Monty, et al. 2007). Very long stream-wise orientated regions of low momentum flanked by regions of high momentum were observed to populate the logarithmic region of all three flows. These features observed in the instantaneous velocity fields had stream-wise extents that exceeded $\Delta x = 20\delta$ and it is thought that a meandering tendency masked the true length from the single point statistics. These events were termed large and very-large scale motions (LSM/VLSM) for pipe and channel flows and ‘Superstructures’ in the boundary layer flow. It was shown that these events carried the bulk of the Reynolds shear stress and over half of the stream-wise turbulent kinetic energy.

The aim of the present work is to study the wall footprint of these events in a fully developed turbulent channel flow. A simultaneous measurement of wall shear stress and velocity was made using a wall normal traversing hot-wire and an array of 10 hot-film shear stress sensors in a fully developed turbulent channel at $Re_\tau = 1000$.

2 Experimental Setup

The channel flow facility is identical to that used in Monty et al. 2007. A row of ten *Dantec 55R47* hot-film sensors ($0.1\text{mm} \times 0.9\text{mm}$ nickel element deposited on $50\mu\text{m}$ thick Kapton foil), were adhered to the channel floor at a distance of $x = 20.55\text{m}$ or $L/h = 205$ from the sand-paper trip (to ensure measurement in a fully developed flow regime). The *Dantec 55R47* sensors were spaced 0.16δ in the

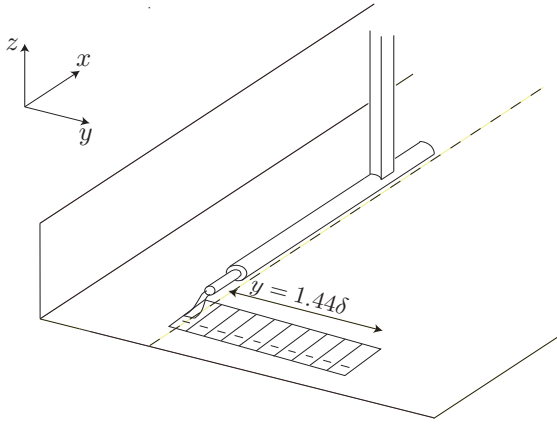


Figure 1: Sketch of hot-film sensor array and arrangement of traversing hot-wire. (Not to scale).

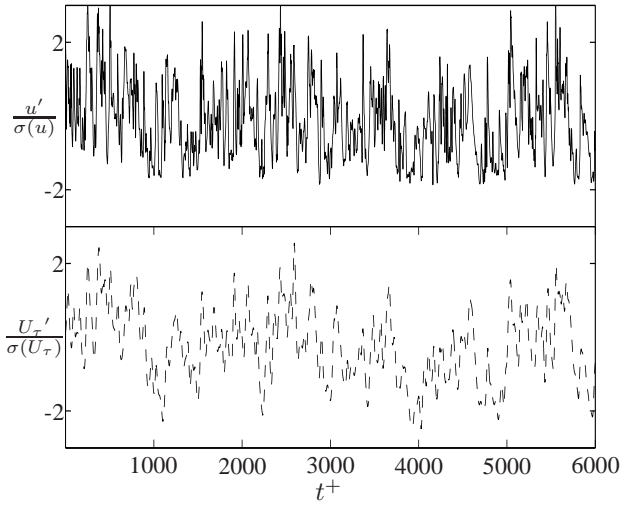


Figure 2: Time series of velocity fluctuation (solid line) from hot-wire located at $z^+ \approx 8$ and time series of shear stress fluctuation (dashed line) from hot-film probe directly under the hot-wire.

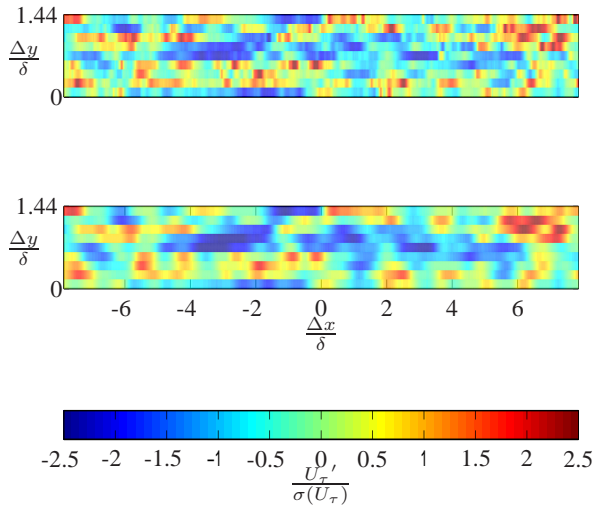


Figure 3: Instantaneous field of the skin friction fluctuation. Top: Raw data. Bottom : A $0.5\delta \times 0.48\delta$ 2-D gaussian filter is applied.

span-wise direction, and this is the minimum spacing that could be achieved given the width of the sensor pad, thus a larger total span ($y = 1.44\delta$) is covered at the expense of span-wise spatial resolution. The stream-wise component of velocity was measured at 40 logarithmically spaced wall normal locations using a traversing hot-wire measuring at the spanwise midpoint of the channel. The hot wire measured from one end of the row of wall mounted hotfilms, thus creating an L-shaped measurement array (see figure 1) covering a domain of $1.44h \times 1.5h$ in the $y - z$ plane. The hot-wire traverse measurement was made using a Dantec 55P05 hot-wire probe ($5\mu\text{m}$ Wollaston wire, etched length = 1mm). This corresponded to $l^+ = lU_\tau/\nu \approx 21$ for $Re_\tau = 1000$. In this paper, x , y and z are the streamwise, spanwise and wall normal directions, with u , v and w denoting the respective fluctuating velocity components. The channel half-height is denoted by h and is interchangeable with δ . Capitalised velocities (e.g. U) or overbars (e.g. \bar{u}) indicate time averages and angled brackets (e.g. $\langle u \rangle$) indicate ensemble averages. Time is denoted by t . The superscript $+$ is used to denote viscous scaling (e.g. $U^+ = U/U_\tau$, $z^+ = zU_\tau/\nu$ and $t^+ = tU_\tau^2/\nu$). δ will be used to denote the boundary layer thickness or channel half-height.

The ten hot-film sensors were operated in constant temperature mode using an *AA Labs AN-1003* hot-wire anemometer. The traversing hot-wire was operated in constant temperature mode using a custom built Melbourne University Constant Temperature Anemometer (MUCTAI). All eleven sensors were simultaneously sampled at a rate of 10kHz which equates to $\Delta t^+ < 1$. The sampling time corresponded to approximately $39000\delta/U_\infty$, and the signatures were recorded in 10 bursts each of 30 seconds duration. All probes were calibrated in situ, with the hot-wire probe calibrated at the channel centre-line using a Pitot-static tube and the hot-film probes were calibrated against the wall friction velocity, U_τ , determined by measuring the pressure drop in the channel. Calibration of the probes was carried out before and after each measurement to ensure that there was no drift due to temperature.

3 Instantaneous fields

Figure 2 shows the time series of fluctuating streamwise velocity from the hot-wire at $z^+ = 8$ and the fluctuating skin friction simultaneously acquired from the hot-film directly under the hot-wire (i.e. $\Delta y = 0$). Although these two signals are remarkably similar, it was found that while the hot-film probes adequately capture the large scale component of the fluctuating wall skin friction, the small scale energy appears attenuated. Possible causes include spatial attenuation owing to the large sensing element

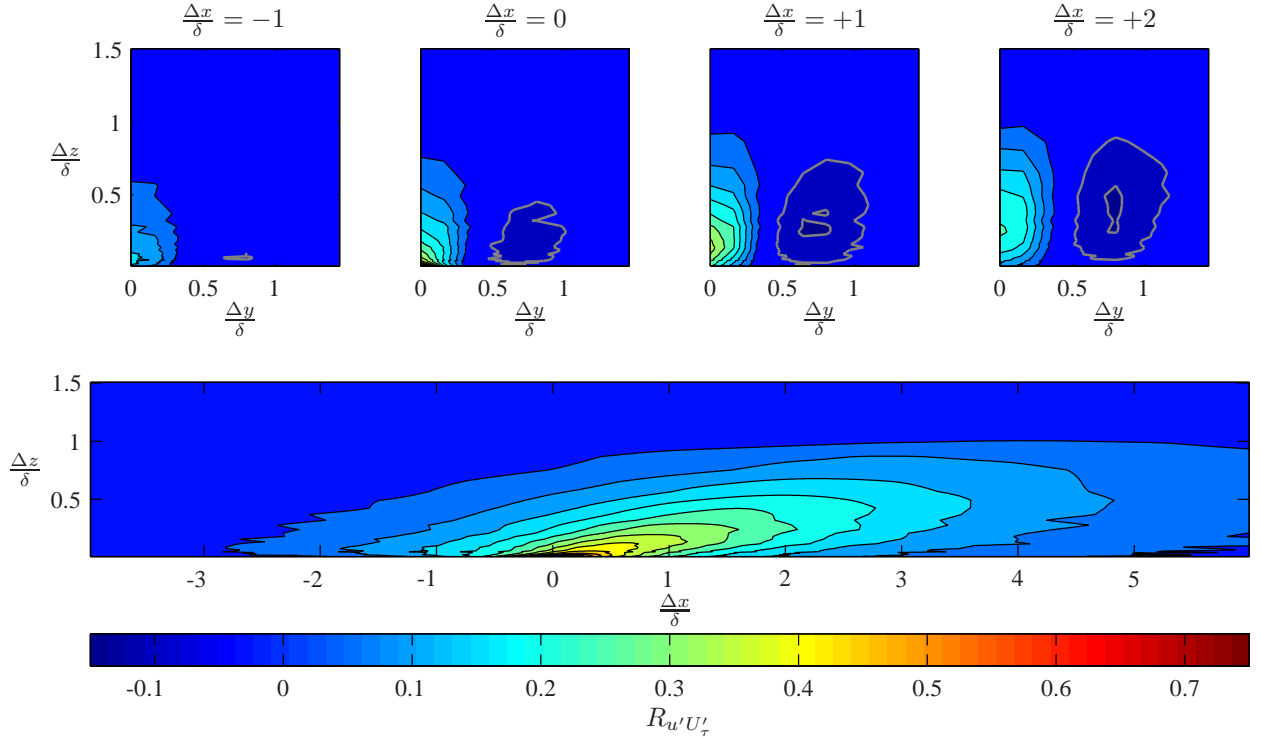


Figure 4: Iso-contours of $R_{u'U'_\tau}$. Two-dimensional views displaying the $x - z$ plane at $\Delta y = 0\delta$ and slices of the $x - z$ plane displayed are four streamwise locations. Contour levels range from -0.15 to 0.75 in increments of 0.05 . Black contours show positive values of $R_{u'U'_\tau}$ and grey contours show negative values.

and also heat loss due to conduction to the wall of the facility. Brunn (1995) discusses these issues in greater detail and also other problems that may be encountered when using these types of wall mounted sensors. Considering that the focus of this study is the wall ‘footprint’ of the *large scale* motions, a two-dimensional gaussian filter spanning $0.5 \times 0.48\delta$ was applied to the hot-film signals to remove the small scale fluctuations. Using data sampled simultaneously from the entire hot-film array, an instantaneous snapshot of the fluctuating wall friction can be projected into the spatial domain using Taylor’s hypothesis. Figure 3 is an example of both the raw and gaussian filtered instantaneous skin friction fields. A convection velocity of $U_c = 0.82U_b$ (see Uddin, et al. 1997) was used to estimate the spatial extent of the large scale fluctuations. This convection velocity was chosen somewhat arbitrarily and further work is required to capture the convection velocity of the large scales at the wall. Nonetheless, elongated regions of alternating low and high shear stress can be observed, which is qualitatively consistent to that reported in (Hutchins & Marusic 2007a) and (Monty et al. 2007) for instantaneous fields of streamwise velocity, however, the streaks of wall skin friction observed here, appear to be shorter than the streaks of velocity reported in those papers.

4 Two-point correlation

The instantaneous fields in figure 3, provide an insight into the size of the ‘footprint’ of the large scale motions, however, they provide no information regarding how the shear stress and the flow structure interact. For a more robust statistical measure, the two-point spatio-temporal correlation of fluctuating velocity, u' , and the fluctuating wall friction velocity, U'_τ , can be computed using:

$$R_{u'U'_\tau}(\Delta t, \Delta y, z) = \frac{\overline{u'(t, z)U'_\tau(\Delta y, t - \Delta\tau)}}{\sigma(u'(t, z))\sigma(U'_\tau(\Delta y, t))}, \quad (1)$$

and again, assuming frozen fields, Taylor’s hypothesis can be used to infer a spatial extent of the correlated region from:

$$R_{u'U'_\tau}(\Delta x, \Delta y, z) = \frac{\overline{u'(\Delta x, z)U'_\tau(\Delta y, x - \Delta x)}}{\sigma(u'(x, z))\sigma(U'_\tau(\Delta y, x))}. \quad (2)$$

The two point correlation has long been used to infer the size and shape of coherent features in turbulent flows. Here, $R_{u'U'_\tau}$, indicates the region of influence of the shear stress on the large scale motions or vice versa. Figure 4 are the contours of $R_{u'U'_\tau}$ and provide a quasi three-dimensional view of the correlated regions in the flow. In the $x - z$ plane, the correlated region is inclined to the wall, leans

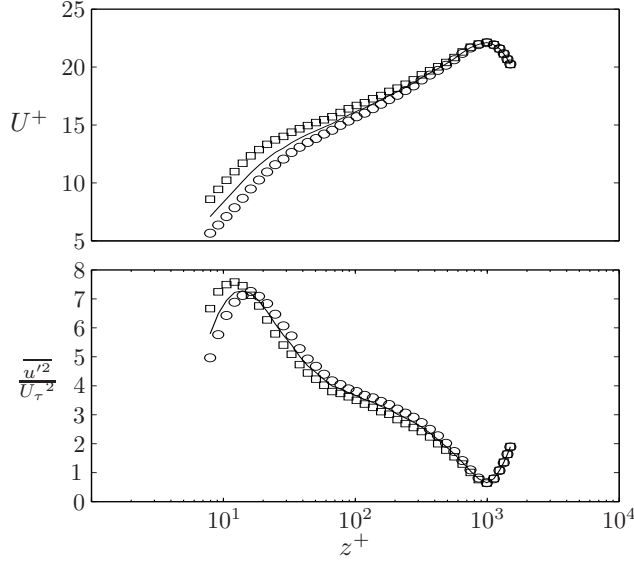


Figure 5: Wall normal profiles of mean velocity and turbulence intensity for (—) unconditional and conditioned on (□) high skin friction and (○) low skin friction.

forward and extends for several δ in the streamwise direction. The correlation is highest nearest the wall at $\Delta x = 0$ and decreases steadily with wall normal distance and streamwise displacement. Slices of the $x - z$ plane for various streamwise positions reveals a negatively correlated region flanking the positively correlated region. The correlated regions of alternating sign indicate that the flow structure is organised in a spanwise alternating pattern. This behaviour is qualitatively consistent with the structure of LSM/VLSM reported in the literature. The magnitude of $R_{u'U_\tau'}$ of the outermost contours is low, yet statistically significant and indicates that a skin friction event is associated with a highly correlated structure which is not only long in the streamwise direction, but also wide in the spanwise direction ($\approx 2\delta$).

5 Conditional Events

The correlation of velocity fluctuations and skin friction, $R_{u'U_\tau'}$, while useful for inferring an average structure size, does not reveal the local behaviour of the flow in the presence of a skin friction event. To investigate these events in isolation, the ensemble averages of velocity and streamwise turbulent kinetic energy were computed based on the presence of either high skin friction ($U_\tau' > 0$) or low skin friction ($U_\tau' < 0$). Since the skin friction and velocity signals are acquired simultaneously, the ensemble average of velocity for low shear stress is computed using;

$$\langle u' |_L(\Delta t, \Delta y, z) \rangle = \langle u' | U_\tau'(t - \Delta\tau, y - \Delta y) < 0 \rangle, \quad (3)$$

and for the turbulence intensity;

$$\langle u'^2 |_L(\Delta t, \Delta y, z) \rangle = \langle u'^2 | U_\tau'(t - \Delta\tau, y - \Delta y) < 0 \rangle. \quad (4)$$

Again projecting the temporal information into the spatial domain using Taylor's hypothesis yields the following equations for ensemble average velocity and turbulent kinetic energy respectively;

$$\langle u' |_L(\Delta x, \Delta y, z) \rangle = \langle u' | U_\tau'(x - \Delta x, y - \Delta y) < 0 \rangle, \quad (5)$$

$$\langle u'^2 |_L(\Delta x, \Delta y, z) \rangle = \langle u'^2 | U_\tau'(x - \Delta x, y - \Delta y) < 0 \rangle. \quad (6)$$

Events computed using a positive shear stress will simply be;

$$\langle u' |_H(\Delta x, \Delta y, z) \rangle = \langle u' | U_\tau'(x - \Delta x, y - \Delta y) > 0 \rangle, \quad (7)$$

$$\langle u'^2 |_H(\Delta x, \Delta y, z) \rangle = \langle u'^2 | U_\tau'(x - \Delta x, y - \Delta y) > 0 \rangle. \quad (8)$$

The ensemble averaged mean velocity profiles and ensemble averaged turbulence intensity profiles (at $\Delta y = 0, \Delta x = 0$) conditioned on low and high skin friction are presented in figure 5. By comparing to the unconditional profiles, one finds that the mean velocity is reduced in the presence of low shear stress and the opposite is true in the presence of high shear stress. The turbulence intensity, however, exhibits a different behaviour. In the presence of low skin friction, the turbulence intensity is reduced when near the wall, yet from approximately $z^+ = 15$ onwards, the turbulence intensity is increased, and remains so until the channel centreline. This behaviour is mirrored in the presence of high skin friction.

The traversing hot-wire probe in combination with the ten hot-film probes can be used to construct a quasi-three-dimensional view of a conditional event. Again, streamwise displacements are estimated using Taylor's hypothesis. It was found that the conditional events were mirrored when switching from low to high skin friction as the conditioning parameter, therefore, only results conditioned on low skin friction are presented here.

In figures 6 and 7, solid line contours show the change in U^+ and the color contours show the corresponding percentage change in turbulence intensity conditioned on low skin friction. Figure 6 has linear wall normal scaling and figure 7 has logarithmic wall normal scaling. The grey contours represent decreased velocity and black contours represent increased velocity. This region of reduced momentum, flanked by high momentum is the signature of the large scale conditional event in the presence of low skin friction. The low momentum region extends 2δ upstream and 4δ downstream of the skin friction event and also extends into the outer region. Slices of the

$y - z$ plane reveals the downstream development of the conditional structure. It is clear that the central low momentum region is flanked by a region of high momentum. The size, shape and spanwise orientation of the conditional structure is very similar to that computed using the two-point correlation. As expected, the strongest deficit in the velocity exists at a streamwise location of $\Delta x = 0\delta$. However, the minimum in ΔU^+ is located above the skin friction event at approximately $z^+ = 15$. This behaviour is inconsistent with the two-point correlation where the magnitude of $R_{u'U'_\tau}$ is highest closest to the wall.

The turbulent kinetic energy appears to be modulated by the presence of a conditional event. Near the wall, the energy is locally attenuated when conditioned on low skin friction, however, when moving away from the wall, the energy modulation switches from attenuation (blue contours) to amplification (red contours). The demarcation separating the region of attenuation and amplification appears to be a function of both streamwise location and wall-normal distance. This boundary appears to approximately coincide with the locus of minima in the conditionally averaged velocity. This is plotted as the black dashed line in both the lower panels of figure 6 and 7. In essence, this locus of minima would divide the conditional flow structure into regions of local streamwise deceleration and local streamwise acceleration. Upstream of the dashed line, the flow decelerates heading towards the low skin friction event and downstream of the dashed line, the flow accelerates away from the low skin friction event. This suggests that a local deceleration is associated with an increase in kinetic energy and local acceleration is associated with a decrease in kinetic energy. This behaviour in the turbulent kinetic energy appears to have a spanwise organisation depending on the sign of the conditional structure. The y - z planes in figures 6 and 7 show that within the high momentum region flanking the central low momentum region, the modulation of the kinetic energy takes on the opposite behaviour as that of a low momentum zone. This is consistent with local acceleration being associated with attenuation of the kinetic energy and local deceleration being associated with amplified kinetic energy.

Although only the streamwise components of velocity and skin friction are measured in this study, it is thought that the behaviour observed in these conditional events may be explained with a counter-rotating roll mode as postulated in Hutchins & Marusic (2007b). According to Hutchins & Marusic (2007b), the counter-rotating roll mode associated with low speed events lifts low speed, energetic fluid away from the wall and the mode associated with high speed events propels high speed, less energetic fluid towards the wall. Here, a low speed structure flanked by high

speed structures forms in the presence of a low skin friction event.

6 Conclusions

Using a novel array of glue-on hotfilm probes and a traversing hot-wire in a fully developed turbulent channel flow, a quasi-three-dimensional view of large scale structures conditioned on large scale skin friction events was investigated. The two point correlation of skin friction and streamwise velocity indicate that the influence of the shear stress on large scale motions or vice versa has a significant extent in both streamwise and wall normal directions and there appears a spanwise organisation consistent with what is reported for LSM/VLSM in the literature. Ensemble averaged velocity and turbulent kinetic energy fields revealed that an inclined, elongated region of low momentum flanked by high momentum is associated with low skin friction with the converse true in the presence of high skin friction. It was found that local deceleration within these conditional structures is associated with an amplification of the turbulent kinetic energy and local acceleration within this region is associated with attenuation of the kinetic energy.

References

- Balakumar B.J. and Adrian R.J. (2007), Large and very large-scale motions in channel and boundary-layer flows. *Phil. Trans. R. Soc. A*, Vol. 365, pp. 665-681.
- Brown G.L. and Thomas A.S.W. (1977), Large structure in a turbulent boundary layer. *Physics of Fluids*, Vol. 20 (10), pp. 243-252.
- Brunn H.H. (1995), *Hot-wire anemometry*, Oxford University Press.
- Guala M., Hommema S.E. and Adrian R.J. (2006), Large-scale and very-large-scale motions in turbulent pipe flow. *Journal of Fluid Mechanics*, Vol. 554, pp. 521-542.
- Hutchins N. and Marusic I. (2007), Evidence of very long meandering features in the logarithmic region of turbulent boundary layers. *Journal of Fluid Mechanics*, Vol. 579, pp. 1-28.
- Hutchins N. and Marusic I. (2007a), Large-scale influences in near-wall turbulence. *Phil. Trans. R. Soc. A*, Vol. 365, pp. 647-664.
- Kim K.C. and Adrian R.J. (1999), Very large-scale motion in the outer layer. *Physics of Fluids*, Vol. 11 (2), pp. 417-422.
- Monty J.P., Stewart J.A., Williams R.C. and Chong M.S. (2007), Large-scale features in turbulent pipe and channel flows. *Journal of Fluid Mechanics*, Vol. 589, pp. 147-156.
- Uddin A.K.M., Perry A.E. and Marusic I. (1997), Experimental investigation of coherent structures in turbulent boundary layers. *J. Mech. Res. Dev.*, Vol. 19 (20), pp. 57-66.
- Wark C.E. and Nagib H.M. (1991), Experimental investigation of coherent structures in turbulent boundary layers. *Journal of Fluid Mechanics*, Vol. 230, pp. 183-208.

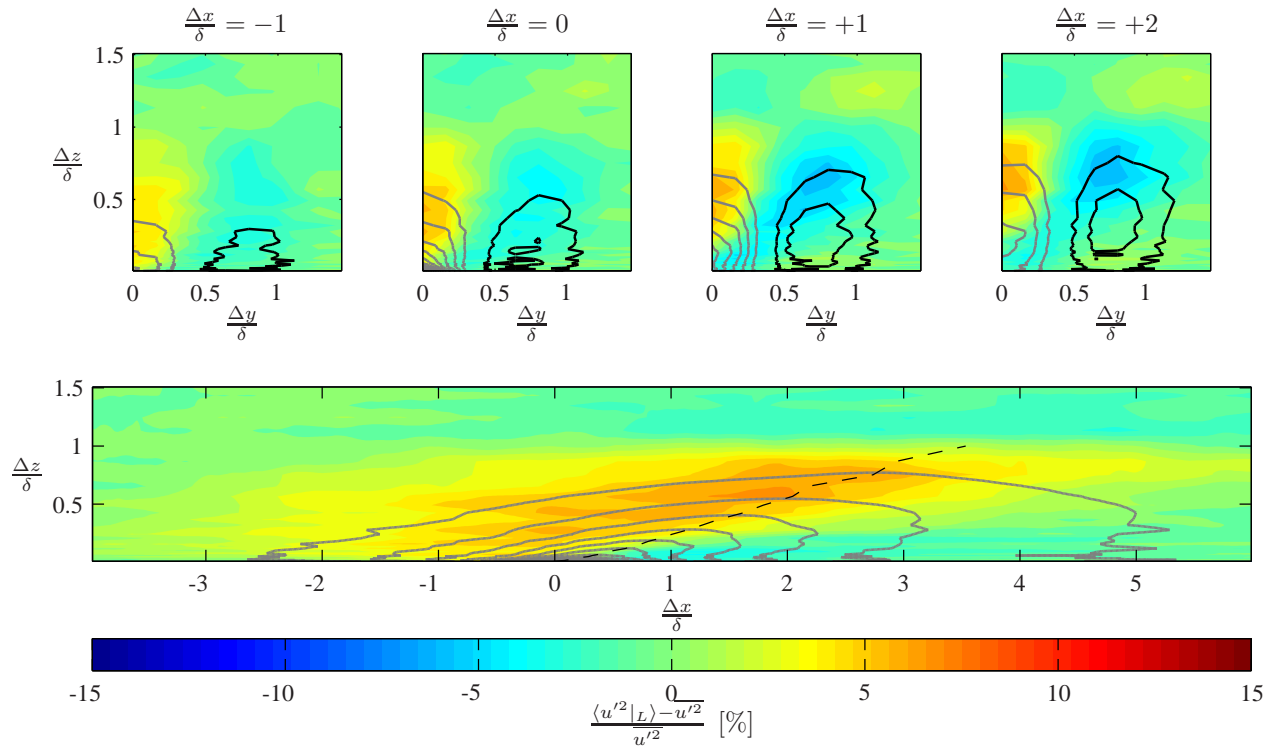


Figure 6: Two-dimensional views displaying the $x-z$ plane at $\Delta y = 0\delta$ and slices of the $x-z$ plane displayed at four streamwise locations for events conditioned on low skin friction. Colour-contours represent the percentage change of the turbulent kinetic energy $(\langle \bar{u}'^2 |_L \rangle - \bar{u}'^2) / \bar{u}'^2$ [%]. Solid contours are the ensemble averaged difference in velocity $(\langle \bar{u} |_L \rangle - \bar{u}) / U_\tau$. Contours lines of $(\langle \bar{u} |_L \rangle - \bar{u}) / U_\tau$ range from -1.6 to 0.15 in 0.15 increments, where grey lines denote negative values and black lines are positive values. Dashed black line is locus of minima in conditional velocity.

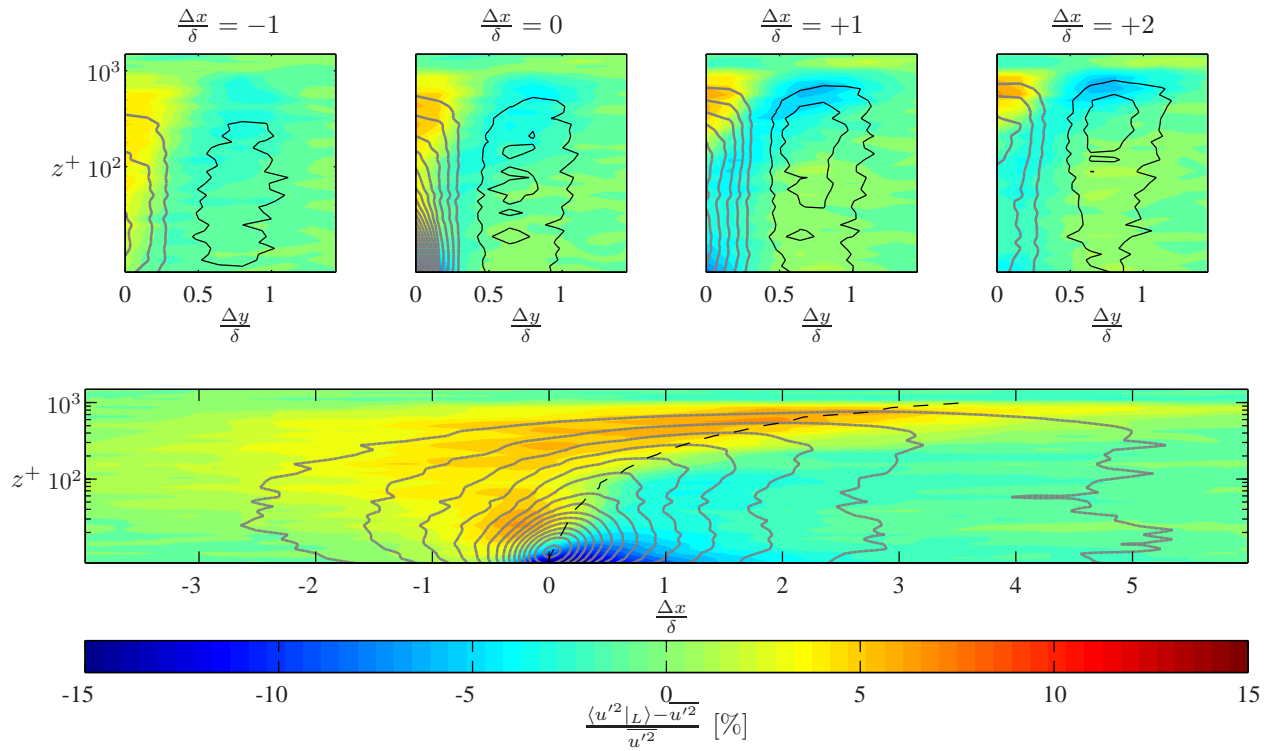


Figure 7: Identical to figure 6 except z -axis is logarithmically scaled to accentuate the near wall behaviour.